Mar. Sci. Tech. Bull. (2023) 12(3): 267-281
e–ISSN: 2147–9666
info@masteb.com

dergipark.org.tr/en/pub/masteb
www.masteb.com
DOI: 10.33714/masteb.1313638

Marine Science and Technology Bulletin

https://prensip.gen.tr/

RESEARCH ARTICLE

Effect of electric vehicle transportation and carbon capture system on concept Ro-Ro ship stability and EEDI

Burak Göksu[1] • Kubilay Bayramoglu[1*]

[1] *Zonguldak Bulent Ecevit University, Maritime Faculty, Department of Marine Engineering, 67300, Zonguldak, Türkiye*

ARTICLE INFO

Article History:
Received: 13.06.2023
Received in revised form: 30.07.2023
Accepted: 08.08.2023
Available online: 28.09.2023

Keywords:
Carbon capture
EEDI
Electric vehicles
Ro-Ro
Stability

ABSTRACT

In terms of their service life, ships may operate for decades. Hence, it depicts the rapid development of machinery and equipment due to the substantial advancement of technology. Indeed, the ship's systems must be updated to accommodate these new instruments. However, the importance of investigating the static-dynamic equilibrium and speed-power demand is a matter of concern as the ships are in motion on the water. There are currently limitations on carbon emissions from ships. To comply with these regulations, either the use of fuels that produce fewer carbon emissions or the use of after-treatment techniques to prevent the release of carbon into the atmosphere are employed. The difficulty of integrating any new system into an existing ship increases the scope of the renovation. This study compares the stability, speed-power, and EEDI values of today's most popular electric vehicles while being transported on a concept Ro-Ro ship with and without a Carbon Capture System (CCS) ship. In the scenario where the ship transports both conventional and electric vehicles, the number of vehicles transported remains constant, but the effects of electric vehicles being heavier are illustrated. A ship with CCS and loaded with electric vehicles has 23.5% less maximum GZ than a regular ship with the traditional vehicles loaded condition by approximately 6% less at an angle of heeling. Also, the EEDI level is approximately one-twentieth of the conventional model, which is an advantage of CCS.

Please cite this paper as follows:

Göksu, B., & Bayramoglu, K. (2023). Effect of electric vehicle transportation and carbon capture system on concept Ro-Ro ship stability and EEDI. *Marine Science and Technology Bulletin*, *12*(3), 267-281. https://doi.org/10.33714/masteb.1313638

* Corresponding author
E-mail address: kubilay.bayramoglu@beun.edu.tr (K. Bayramoglu)

Introduction

Car carriers are ships designed to transport automobiles, lorries, buses, and other wheeled vehicles in combinations (Kang et al., 2012). Roll-on, roll-off (Ro-Ro) ships are a type of these vessels because the loading and unloading processes are similar as well. Pure Car Carriers (PCC) are vessels that transport only cars, whereas Pure Car Truck Carriers (PCTC) transport other forms of wheeled cargo (Yasukawa, 2019). In addition to cargo ships, there are several other varieties of Ro-Ro ships, including ferries and even military tanks (Kennedy, 2023).

Car carriers load and unload without cranes or pumps, unlike other ships. The ramps, usually at the ship's stern or stem (rarely on the side), allow wheeled vehicles to be moved to their specified spots on the ship, and the cargo is unloaded at the planned port by reversing the procedure (Tuswan et al., 2021). It has a different load capacity measurement standard, such as DWT on cargo ships and TEU (Twenty Foot Equivalent Units) on container ships, the total loading length in lanes on Ro-Ro ships, or the total number of vehicles it transports (Sun et al., 2022). The greatest Pure Car Carrier (Höegh Target) is capable of transporting up to 8500 cars on fourteen distinct decks and is designed for trade between East Asia and Europe (Nieuwenhuis, 2017). Despite its highest payload, this ship is not the longest vehicle carrier because it is approximately 200 meters long and 36 meters wide.

Car carriers are readily identifiable from the exterior due to their conspicuously elevated sideboards (Simopoulos et al., 2008). Due to the large surface area of their sides, ships are susceptible to drifting off course in strong winds (Thies & Ringsberg, 2023). Stacking decks on top of each other increases the transport capacity of the vehicle. To prevent cargo space loss, tween decks are arranged to attain maximum loading capacity (Skoupas et al., 2009). In addition, two ramps, one at the bow and one at the stern, are utilized to complete loading and unloading in the shortest amount of time feasible (Sun et al., 2022).

In the atmosphere, gases that absorb and emanate infrared radiation from the sun are referred to as Greenhouse Gases due to their effect (Kavli et al., 2017). Although these gases occur naturally in the atmosphere, variations in their concentrations caused by human activities contribute to global warming (Salinger, 2005). Carbon dioxide has the largest proportion of the greenhouse gases that contribute to global warming (Zhong & Haigh, 2013). Carbon dioxide accounts for the largest portion of greenhouse gas emissions at 74.4%, followed by methane at 17.3% (Shepherd et al., 2015). Others include nitrous oxide, sulfur hexafluoride, hydrofluorocarbons, perfluorocarbons, and NF_3 (nitrogen trifluoride) (Zhou & Feng, 2014). The primary causes of the global increase in greenhouse gas emissions are listed as fossil fuel use (87%), Land-use-related forest loss (9%), industrial processes (4%), breathing, decomposition and dissolution mechanisms, natural causes, ocean discharge, and anthropogenic causes (Mikhaylov et al., 2020).

In addition to these, greenhouse gases are responsible for the fact that the Earth is not a frozen sphere (Kweku et al., 2017). Without the greenhouse effect, the average temperature on Earth would have decreased from 14 degrees Celsius to -18 degrees Celsius (McClintock et al., 2008). Human actions like the natural greenhouse effect have increased greenhouse gas accumulations in the atmosphere, raising global surface temperatures and causing climate change.

The most well-known carbon emission regulation is the Paris Agreement. The aim of the legislation signed by 196 countries on December 12, 2015, is to limit global warming to less than 2 degrees Celsius, preferably 1.5 degrees Celsius (Sachs, 2020). This corresponds to levels before the industrial revolution. The European Green Agreement signed in 2019 sets the goal of reducing EU country emissions by 55 percent by 2030 compared to 1990 and achieving carbon neutrality by 2050 (Perissi & Jones, 2022).

The International Maritime Organization (IMO) has enacted various regulations to decrease carbon emissions from ships. The rules were first put in place in 2008. It also tries to cut carbon emissions gradually (Wang et al., 2021). The main aim is to cut GHG emissions by approximately 50% by 2050 compared to 2008 (Issa et al., 2022). The IMO attempts to meet these goals through a variety of regulations. The regulations became implemented as part of MARPOL Annex VI, primarily aimed to reduce air pollution from ships (IMO, 2022). These standards are the Energy Efficiency Design Index (EEDI), Energy Efficiency Existing Ship Index (EEXI), Energy Efficiency Operational Index (EEOI), Ship Energy Efficiency Management Plan (SEEMP), and Carbon Intensity Index (CII). EEDI attempts to reduce CO_2 emissions per unit of transport by improving ship-carrying capacity during the building phase or by implementing measures to improve energy efficiency (Polakis et al., 2019). EEXI "describes standardized CO_2 emissions based on installed engine power, cargo capacity, and ship speed" and "identifies CO_2 emissions per cargo ton and transport." In other terms, the EEXI establishes a CO_2 emission limit per unit of transportation supply (Rutherford et al., 2020).

New and existing ships must keep a ship-specific Ship Energy Efficiency Management Plan (SEEMP) that can be linked to the Safety Management System. SEEMP will be IMO-compliant. The January 1, 2013 requirements apply to all vessels with a gross tonnage of 400 or greater (Hasan, 2011).

Emissions from ships depend on numerous other variables, such as the fuel type, the ship's machinery, cruising duration, cruising speed, and occupancy rate (Tadros et al., 2022). Low- and medium-speed diesel engines, as well as steam and gas turbine engines to a lesser extent, are what power the majority of commercial vessels (Mihail–Vlad, 2018). In marine shipping, fossil fuels are used in ship machinery. The ecology and human health suffer from these emissions. If we call the pollution seen in people's immediate environment, such as inland water, narrow channels, gulfs, ports, beaches, and seashore settlements, pollution of the immediate environment, we can also refer to the pollution we don't notice but that has global effects on our environment. It's also termed global environmental contamination. Principal forms of emissions from commercial ships are carbon dioxide (CO_2), carbon monoxide (CO), sulfur oxides (SO_X), nitrogen oxides (NO_X), hydrogen chloride (HC), dust or particulate matter (PM), and organic volatile vapors and gases (VOC) (Xing et al., 2020).

In regions with dense ship traffic, emissions from ships are concentrated, and measures are taken to reduce and keep them under control (Ampah et al., 2021). With the implementation of MARPOL Annex VI, the International Maritime Organization (IMO) has enacted several regulations regarding ship emissions of exhaust gases. Many standards regarding nitrogen oxides (NO_X), sulfur oxides (SO_X), and particulate matter are still in effect, assisting to improve air quality.

Ship CO_2 emissions are reduced in several ways. These apps fall under three categories. First, it reduces engine power through energy efficiency. These applications generally involve waste heat recovery, propeller and rudder design optimization, hull shape, and hull pollution (Bøckmann & Steen, 2016). Second, use alternate ship fuels. After 2030, hydrogen and ammonia will replace LNG as ship fuels (Fayaz et al., 2012; Law et al., 2023; Shin & Park, 2023). Finally, if renewable energy sources or alternative fuels are to be used, it is thought that carbon capture systems will have a significant impact on reaching the 2050 IMO targets (Lee et al., 2021).

Since electric vehicles are today's new technology products, they must be transported from the production place to the consumption location. This necessitates an evaluation of both the stability of current ships and compliance with the regulations limiting greenhouse gas emissions, which are primarily caused by the transportation of ships and vehicles and represent the novelty of the study. In this study, the transportation of electric vehicles on Ro-Ro ships was evaluated instead of vehicles using traditional fossil fuels, which play an important role in reducing greenhouse gases. The effects of carrying electric vehicles instead of conventional vehicles on ship stability were explored in the studies. Furthermore, the effect of carbon capture systems on Ro-Ro ship applications on ship stability and EEDI has been assessed for various scenarios. Carbon capture systems are one of the most effective techniques for lowering CO_2 emissions in line with IMO 2050 targets. In this context, the following sections of this study perform EEDI and stability calculations both in the presence and absence of electric vehicles and with and without CCS. Thus, the combined application of electric vehicle transport and carbon capture systems in Ro-Ro ships will be evaluated, which has not been performed before in the literature.

Material and Method

General Specifications of the Concept Ship

A concept design of a PCC-type Ro-Ro ship has been modeled, and features such as the main engine power and type, which are determined based on the approximate calculation of the general weight groups, hydrostatic and stability values, and resistance-power calculations, are completed within the scope of the ship's preliminary design calculations. When calculating stability and resistance power, it is presumed that the ship floats in two drafts, 10.50 m, and 11.11 m. The 10.50 m water draft is required to transport vehicles that have conventional engines. The 11.11 m water draft is required if the entire cargo consists of new-generation electric vehicles. In addition, stability calculations were performed for both the presence and absence of carbon capture equipment, considering that waterlines remained unchanged. Consequently, the resistance-power calculation comprises two combinations, while the stability calculation comprises four. The fundamental characteristics of the ship are detailed in Table 1.

The concept design PCC Ro-Ro ship has 14 vehicle decks and allows for the loading of a total of 7700 cars. The overall design of the ship designed within the scope of this study is depicted in Figure 1, and it is designed to have a conventional propulsion system consisting of a single internal combustion main engine and a propeller.

The weight groups of the ship were calculated using empirical formulas from the literature, and the method of estimating values based on empirical formulas is frequently

used within the preliminary design phase of ship construction. In Table 2, weight categories, empirical weight estimation methodologies, and values are listed.

Thus, the weight groups and distributions of the ship, as well as its general characteristics, determine its total displacement. This factor is of the utmost significance when calculating resistance-power, and stability, and it is an indispensable aspect of ship design.

Table 1. The concept ship general specifications

Specifications	Values	
Length overall (LOA) [m]	230.0	230.0
Draft Amidships (T) [m]	10.50	11.11
Displacement [t]	53050	56900
Waterline (WL) Length [m]	219.99	220.25
Beam max extents on WL [m]	32.00	32.00
Wetted Area [m²]	8991.1	9300.9
Waterplane Area [m²]	6189.9	6268.9
Prismatic coefficient (Cp)	0.748	0.755
Block coefficient (Cb)	0.700	0.707
Max Section area coefficient (Cm)	0.945	0.948
Waterpl. area coeff. (Cwp)	0.879	0.890

Carbon Capture System (CCS) Specifications

CO_2 emissions are the main contributor to global warming and the greenhouse effect. Carbon capture systems are the most effective approach for reducing CO_2 emissions from ships (M. Wang et al., 2011). Figure 2 shows a carbon capture system and the tanks used to store the stored carbon.

The system consists of a carbon capture column that Absorbs the CO_2 components in the diesel engine exhaust gas, a Stripper that separates the CO_2 from the rich MEA solution, and tanks that store the liquefied CO_2 emissions under high-pressure and low-temperature conditions. Considering the literature data, the optimum operating condition of the CCS system is 45-55 degrees. In this study, it is thought that the exhaust temperature enters the CCS system at 50°C. The reduction of the exhaust gas to these temperatures is generally provided by waste heat recovery systems or scrubber systems (Mores, Rodríguez, et al., 2012; Mores, Scenna, et al., 2012).

Considering the power requirement of the Ro-Ro ship, Considering the power requirements of the Ro-Ro ship, the MAN brand 8S60ME-C10.6 main engine, which produces 19600 kW at full load, was chosen (MAN, 2017). The marine diesel engine used in this study specification is presented in Table 3.

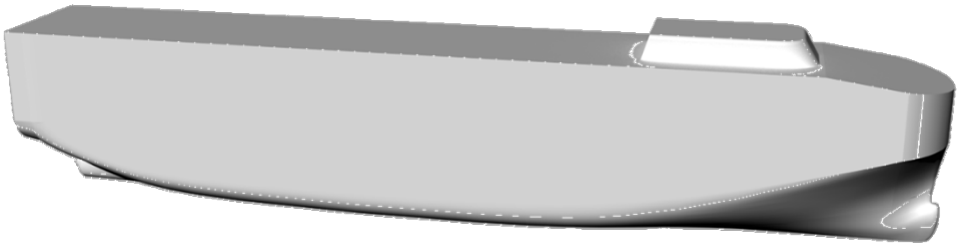

Figure 1. The general view of the concept ship

Table 2. The weight groups, methodologies, and weight values

Weight group	Calculation method	Weight [t]	
		T=10.50 m	T=11.11 m
Construction	Kafalı (1988)	20000	
Main machinery	Barrass (2004)	1800	
Auxiliary machinery	Kupras (1981)	1000	
Outfitting	Kafalı (1988)	4500	
Engine car cargo load	Jia (2007)	11550	-
Electrical car cargo load	Kane (2023)	-	15400
Service requirements	Sun et al. (2022)	14200	
Displacement		25750	29600
Total displacement		53050	56900

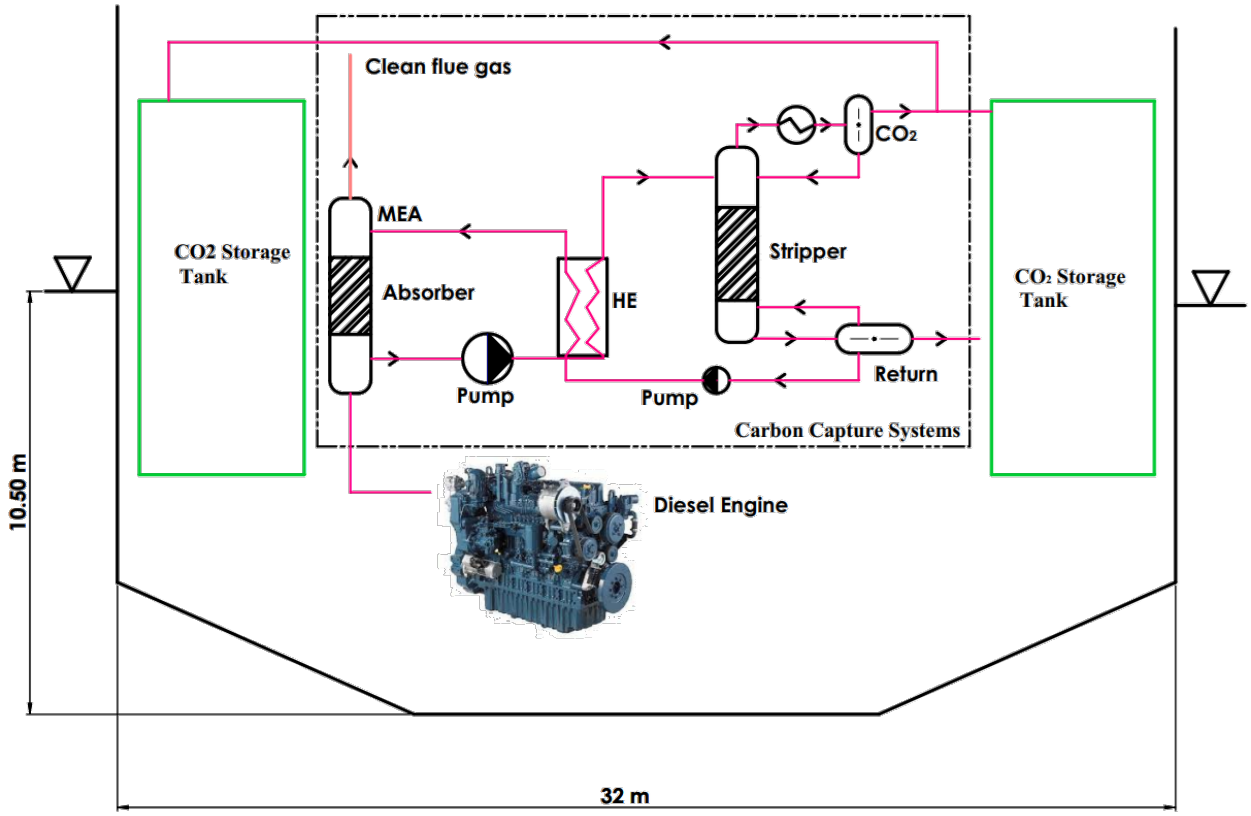

Figure 2. Carbon capture systems on board

Table 3. Specification of diesel engine (unit: kg/s)

Load	Exhaust Mass Flow Rate
100	38.7
85	35.6
75	32.8
50	22.8
25	14

Table 4 summarizes the fractional ratios of the gases in the exhaust gas. Components represent approximate values (Stec et al., 2021).

Table 4. Flue gas composition of diesel engine (unit: Vol%)

Exhaust Gas Composition	Value
H_2O	13
CO_2	12
O_2	3
N_2	72

Stability Parameters

The equilibrium of forces acting on floating bodies like ships has revealed the existence of numerous stability control parameters (Im & Choe, 2021). The expression "metacenter height", which is used to determine initial stability, is the most fundamental of these concepts (Ibrahim & Grace, 2010). This variable term is calculated based on conditions such as displacement, hell, and trim angle. To achieve equilibrium, the sum of an object's forces and moments must be zero. The center of buoyancy and center of gravity of a ship without a heel is in the same direction. If a change occurs that causes the distance between these centers to be greater than zero, the heel motion is observed until the directions of the ship's center of buoyancy and center of gravity are the same again (Shakeel et al., 2022). In this new equilibrium state, the point depicted in Figure 3 that passes from the new buoyancy center of the ship perpendicular to the "B" waterline and intersects the ship's center line is known as the "metacenter point" "M". The distance between the ship's center of gravity "G" and this point "M" on the center line is the ship's "GM" value. This value is a parameter evaluated within the scope of IMO intact stability rules, and stability is mentioned when it is greater than zero (Marlantes et al., 2022). If not, the ship cannot satisfy the floating condition.

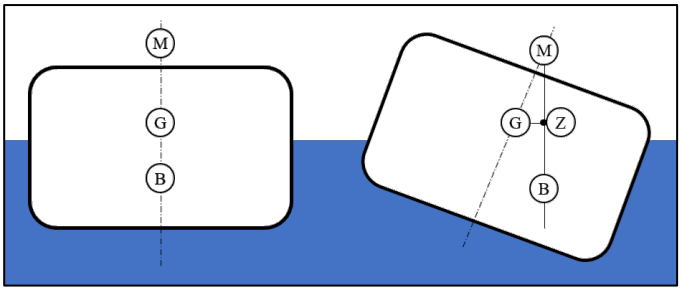

Figure 3. Ship initial stability condition

The term "righting arm – (GZ)" is also utilized when evaluating the stability of ships (Perrault, 2016). The vertical distance from the ship's center of gravity to the line that passes through B and M and intersects this line at the "Z" point, which serves as the moment arm, depends on the heel angle of the ship. The ships return to their prior positions and assume the initial position because of the moment arm formed here.

Figure 4 shows three patterns of the area under the GZ curve in the IMO stability regulation. The $area_{0\text{-}30deg}$ refers to the area of "a" under the GZ curve between 0 and 30 of the heeling angle, the $Area_{30\text{-}40deg}$ is the area of "b" between 30 and 40 (or flooding angle, whichever is less) and the $Area_{0\text{-}40deg}$ means the area of "a+b" between 0 and 40 (or flooding angle, whichever is less) (Im & Choe, 2021). A typical $GZ - \varphi$ curve has a positive value within a certain range of heeling angles, and the heeling angle at which the value of the curve changes from positive to negative is known as the "stall angle" (Göksu & Bayramoğlu, 2021). When the heel angle exceeds this value, a swaying moment arm forms instead of a righting moment arm, resulting in a ship capsizing. Cargo and passenger ships are required by IMO regulations to meet some criteria. However, ships that meet these stability values are allowed to operate at sea and are physically tested to meet this criterion by means such as strict controls and inclination tests (Irkal et al., 2016).

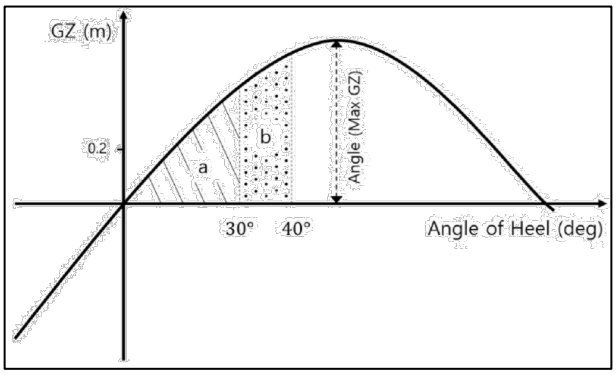

Figure 4. A typical GZ-φ graph (Im & Choe, 2021)

Resistance-Power Calculations

Estimating the resistance of the hull form is one of the most crucial design parameters in ship design (Labanti et al., 2016). The resistance-power calculation is based on the ship's principal parameters, which vary based on the type of ship being calculated and its geometrical characteristics. In the first stage, empirical formulations are utilized, which are typically derived from the results of numerous systematic model experiments and statistical research (Niklas & Pruszko, 2019). The precision of the calculation to be performed using the theoretical method depends on the similarity between the chosen method's underlying form and the form available. The arrangement of the method, which J. Holtrop created in 1977 with assistance from G. G. Mennen in 1978, has allowed the Holtrop-Mennen method (Song et al., 2013), which developed on the foundation of conventional cargo ships (Korlak, 2021).

Total ship resistance is expressed as the sum of several resistance components, and Equation (1) incorporates the resistance components used when transforming from model tests to full-scale ship scale (Holtrop & Mennen, 1982; Molland et al., 2017).

$$R_T = R_F(1 + k_1) + R_{APP} + R_W + R_B + R_{Tr} + R_A \quad (1)$$

where R_T is the total resistance of the ship; R_F is friction resistance according to ITTC, $1 + k_1$ form factor, R_{APP} is the resistance of attachments, R_W is wave making and wave breaking resistance, R_B is bulb pressure resistance, R_{Tr} is stern pressure resistance, R_A is ship-model adaptation resistance. This equation is the basis of the Holtrop-Mennen method and is one of the most frequently used methods in the shipbuilding preliminary design phase (Grabowska & Szczuko, 2015).

The first step in determining the required installed engine power for ships is to determine the total resistance. Then, the power required to tow a ship at V speed is referred to as P_E and can be calculated using Equation (2) (Molland et al., 2017).

$$P_E = R_T * V \quad (2)$$

Estimating or calculating the amount of power losses that occur on all components from the main engine to the propeller and during propeller rotation is another vital requirement for determining the installed engine power to achieve the necessary thrust from the propeller that propels the ship forward. In this regard, the concept of propulsion efficiency η_T comes into perform, and it is accepted by researchers that 60 percent of the total main machine power is lost on a conventional propulsion system before the power from the main machine is converted into useful power (Charchalis, 2014). In other terms, this issue, also known as the ratio of the hull effective power to the main engine brake power, P_B is illustrated in Equation (3) (Demirel et al., 2017).

$$\eta_T = \frac{P_E}{P_B} \quad (3)$$

Thus, the selection of the main engine that will enable providing a ship where the total force of resistance can be estimated could be made at the specified speed.

Carbon Capture and EEDI Calculations

The carbon capture device considerably lowers CO_2 emissions in a marine diesel engine that uses fossil fuels. To reduce CO_2 emissions from ship exhaust gas, an amine solution is utilized (Luo & Wang, 2017). The CO_2 capture process was simulated using Aspen Plus software. For the equation of state (EOS), the electrolyte non-random two-liquid model (eNRTL) was applied. The law of the Henry constant and the dielectric constant of each component, which are eNRTL parameters, were taken from the literature to determine the equilibrium constants. The CO_2 capture mechanism of activated MEA is expressed by eight equations (Lee et al., 2021). It uses the common 25 wt% percent ethanolamine (MEA) solvent. MEA solvent was used as 25 wt% in this study.

The EEDI expresses the CO_2 emission per unit of transported cargo by the CO_2 released from the ship's main and auxiliary machinery, and it was implemented to reduce CO_2 emissions from ships. Alternative power requirements and heat recovery systems on the ship provide a reduction of CO_2 emissions (Stec et al., 2021). Carbon capture systems play the main role in reducing CO_2 emissions from ships. The EEDI is computed using Equation (4).

$$EEDI = \frac{P_{ME} \cdot C_{F,ME} \cdot SFOC_{ME} + P_{AE} \cdot C_{AE} \cdot SFOC_{AE}}{V_{ref} \cdot Capacity} \quad (4)$$

Where P is engine power expressed in kW, C_F is the ratio of fuel consumption to CO_2 emissions, $_{SFOC}$ is standard fuel oil consumption expressed in g/kWh, V_{ref} is ship speed defined in kn, and capacity is indicated in tons deadweight reported in dwt. The main and auxiliary engines are denoted by the subscripts *ME* and *AE*, respectively. For all of the situations that were examined, SFOC was set at 200 g/kWh according to the literature. Equation (5) can be used to compute the power of auxiliary engines (MAN, 2014).

$$P_{AE} = 0.05 \cdot MCR_{ME} \quad (5)$$

Results and Discussion

Definition of the Stability Parameters

Throughout their voyages, ships are exposed to highly variable conditions. Although the effects of these conditions on the ship were not completely known before that, their safety is maintained if they comply with the stability requirements established by international conventions and approved by classification societies according to their designs. Ships end up sinking or being damaged because of improper cargo or a failure to observe changes in ship equilibrium during a voyage. There are casualties among seafarers, material losses, and extensive marine and environmental damage. Regardless of the type and size of the ship being designed, it is essential to obtain the hydrostatic values table initially. The relevant values for the hydrostatic calculations of the concept PCC Ro-Ro vessel designed for this study are listed in Table 5.

Table 5. Hydrostatic values of the concept ship

Draft Amidships [m]	**9.50**	**10.00**	**10.50**	**11.00**	**11.50**	**12.00**
Displacement [t]	46763	49877	53050	56221	59442	62691
Heel [deg]	0.00	0.00	0.00	0.00	0.00	0.00
Draft at FP [m]	9.50	10.00	10.50	11.00	11.50	12.00
Draft at AP [m]	9.50	10.00	10.50	11.00	11.50	12.00
Draft at LCF [m]	9.50	10.00	10.50	11.00	11.50	12.00
Trim (+ by stern) [m]	0.00	0.00	0.00	0.00	0.00	0.00
WL Length [m]	219.39	218.96	219.99	220.23	220.25	220.31
Beam max extents on WL [m]	32.00	32.00	32.00	32.00	32.00	32.00
Wetted Area [m^2]	8486.68	8731.17	8991.05	9247.34	9497.87	9745.31
Waterplane Area [m^2]	6046.66	6116.79	6189.96	6256.76	6312.67	6361.34
Prismatic coefficient (Cp)	0.737	0.745	0.748	0.754	0.760	0.766
Block coefficient (Cb)	0.684	0.695	0.700	0.708	0.716	0.723
Max Section area coeff. (Cm)	0.939	0.942	0.945	0.948	0.950	0.952
Waterplane area coeff. (Cwp)	0.861	0.873	0.879	0.888	0.896	0.902

Table 6. Loading conditions for all combinations

Item Name	Long. Arm [m]	Vertical Arm [m]	Total Mass (Conv.) [t]	Total Mass (Conv. +CCS) [t]	Total Mass (EVs) [t]	Total Mass (EVs +CCS) [t]
Construction	110.00	10.00	20000.00	20000.00	20000.00	20000.00
Machinery	28.00	3.00	2800.00	2800.00	2800.00	2800.00
Outfitting	110.00	8.00	4500.00	4500.00	4500.00	4500.00
Car deck 1	110.00	2.70	450.00	365.00	600.00	515.00
Car deck 2	110.00	5.00	450.00	365.00	600.00	515.00
Car deck 3	110.00	7.30	525.00	440.00	700.00	615.00
Car deck 4	110.00	9.60	825.00	740.00	1100.00	1015.00
Car deck 5	110.00	11.90	825.00	740.00	1100.00	1015.00
Car deck 6	110.00	14.20	825.00	740.00	1100.00	1015.00
Car deck 7	110.00	16.50	825.00	740.00	1100.00	1015.00
Car deck 8	110.00	18.80	975.00	880.00	1300.00	1210.00
Car deck 9	110.00	21.10	975.00	890.00	1300.00	1210.00
Car deck 10	110.00	23.40	975.00	890.00	1300.00	1215.00
Car deck 11	110.00	25.70	975.00	890.00	1300.00	1215.00
Car deck 12	110.00	28.00	975.00	890.00	1300.00	1215.00
Car deck 13	110.00	30.30	975.00	890.00	1300.00	1215.00
Car deck 14	110.00	32.60	975.00	890.00	1300.00	1215.00
Service req.	115.00	8.00	14200.00	14200.00	14200.00	14200.00
CO_2 storage tank port side	50.00	32.00	0.00	400.00	0.00	400.00
CO_2 storage tank stb. side	50.00	32.00	0.00	400.00	0.00	400.00
Carbon capture system	50.00	32.00	0.00	400.00	0.00	400.00
Total tonnage			53050.00	53050.00	56900.00	56900.00

Note: * "Conv." is for carrying conventionally engined cars; "Conv.+CCS" is for carrying conventionally engined cars with a carbon-captured system ship; "EVs" is for carrying electric vehicles; "EVs+CCS" is for carrying electric vehicles with a carbon-captured system ship.

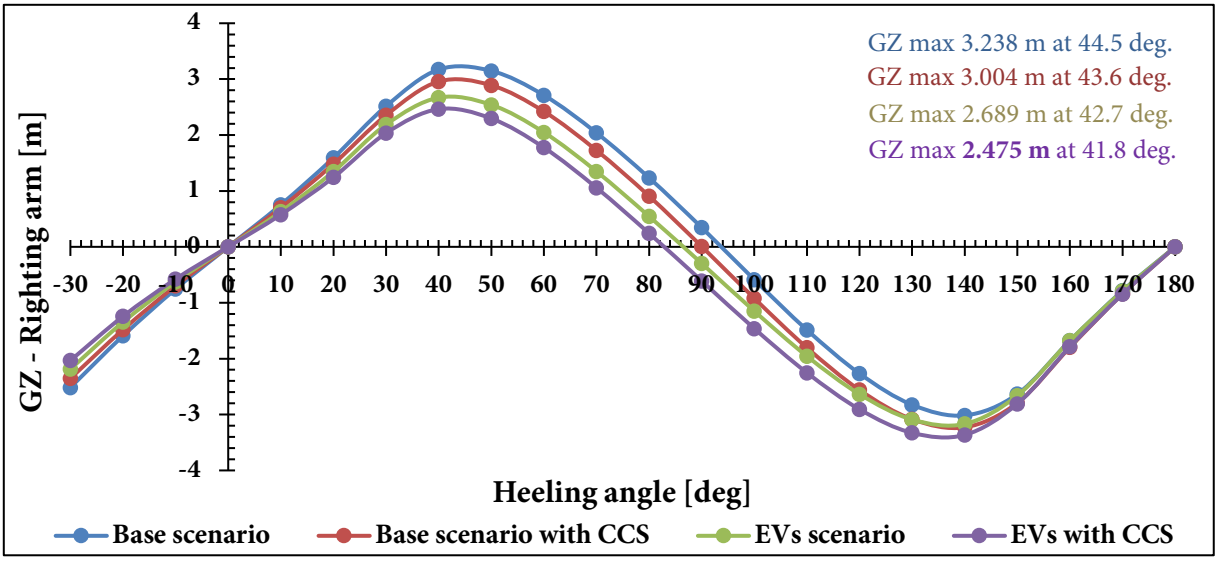

Figure 5. Stability curves for all conditions

A series of calculations must be performed to determine the equilibrium and stability characteristics of a designed ship model. For these calculations, it is necessary to first determine the weight of the ship's hull, machinery, and equipment, the load transported on the decks and holds, the load required for service, and the position of equivalent specialized equipment on the ship's hull. With the data derived from stability calculations and related equilibrium conditions, it is possible to predict the ship's movements in the floating state. Table 6 displays the cargo information for each loading combination of the concept ship. These calculations are also beneficial for developing hull designs.

As depicted in Figure 5, the $GZ - \varphi$ graph must be available to determine if the ship could meet the floating condition at the end of any change caused by internal and external forces acting on the ship; if these forces disappear, the ship can return to its initial equilibrium position. Considering the values obtained for the four distinct loading conditions to be evaluated within the scope of the study, the case where conventional vehicles are carried without CCS has the largest positive stability range and maximum GZ righting arm.

Definition of Resistance-Power Values

The Holtrop-Mennen method was utilized for the resistance calculations of the conceptual ship shape developed. Ship resistance calculations, which are crucial in deciding the main engine type and power during the design phase, are also commonly used to approximately predict the cruising speeds under the decided conditions with the existing main engine. To determine the amount of main engine power that will be needed for propulsion if the propulsion efficiency (η_T) is limited to 40%, and to obtain what speeds the determined form will encounter with what magnitude of resistance, the data in Table 7 can be accessed under two different draft conditions evaluated in the study.

Naturally, increasing the draft, i.e. carrying more cargo, will lead to either a higher main engine power requirement or a slower cruising speed with the same power. So, Figure 6 illustrates the increase in required power as the draft increases for two distinct drafts.

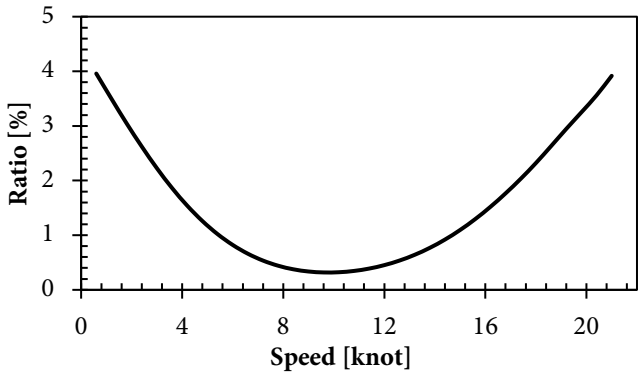

Figure 6. Increase in power by changing speed with the draft from 10.50 to 11.11 m

Table 7. Resistance-Power values for the concept ship at different drafts

Speed (knot)	Draft at 10.50 m		Draft at 11.11 m	
	Resistance (kN)	Power (kW)	Resistance (kN)	Power (kW)
0	--	--	--	--
3.0	28.8	111	29.4	114
6.0	108.7	839	109.6	846
9.0	236.2	2734	237.0	2743
12.0	411.0	6343	412.9	6372
12.6	452.8	7337	455.2	7377
13.2	497.4	8444	500.6	8498
13.8	545.2	9676	549.3	9750
14.4	596.6	11049	602.1	11150
15.0	652.1	12581	659.3	12718
15.6	712.3	14291	721.5	14476
16.2	777.7	16203	789.5	16450
16.8	848.9	18342	863.9	18666
17.4	926.6	20735	945.4	21157
18.0	1011.4	23415	1034.9	23958
18.6	1103.9	26407	1132.9	27102
19.2	1204.3	29737	1239.7	30613
19.8	1313.8	33455	1356.4	34542
20.4	1434.7	37643	1485.8	38983
21.0	1568.4	42360	1629.8	44019

Determination of Carbon Capture and EEDI

The most important factor in carbon capture processes is the choice of solvent to absorb CO_2 emissions. In this study, the MEA solution, which is mostly used in the literature, was used in the system model with 25% MEA and 75% water by weight. In this study, the effect of MEA solution amount on CO_2 reduction performance was investigated under five different engine load exhaust conditions. The effect of MEA at different rates for each load case on the CO_2 reduction performance is given in Figure 7. CCS calculations were made for variable engine loads and corresponding exhaust mass flow rates. The findings show that as the MEA ratio increases, the CO_2 reduction performance increases. However, it was determined that the increased MEA ratio after a certain threshold value did not affect the CO_2 reduction performance. It has been shown that increasing MEA ratio and CO_2 capture performance have the same characteristics for each load condition. In addition, it has been determined that the optimal MEA amount for each load condition is approximately three times the exhaust gas flow rate.

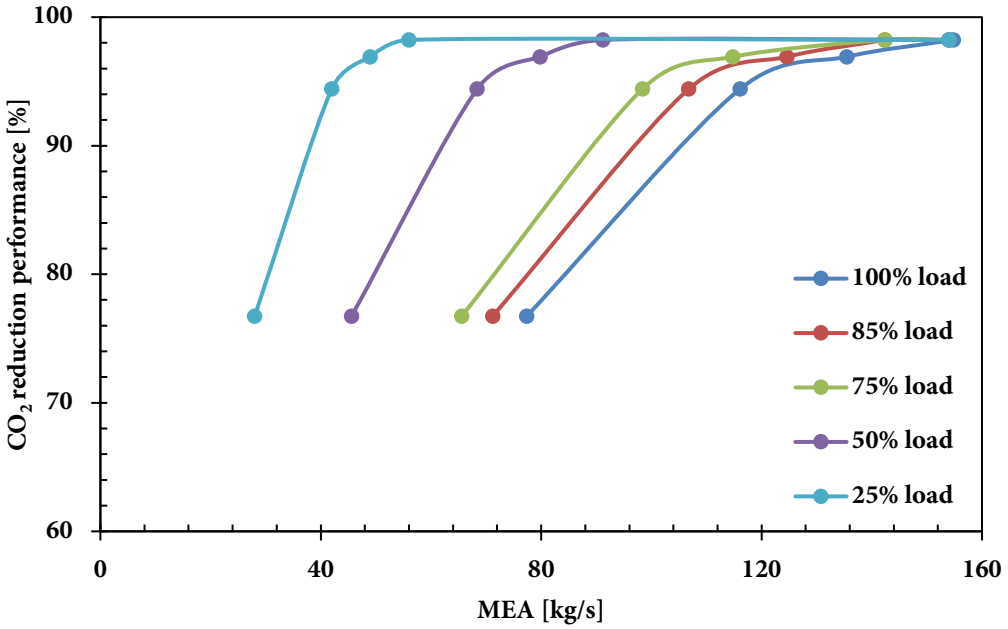

Figure 7. Effect of MEA solution amount on CO_2 reduction performance

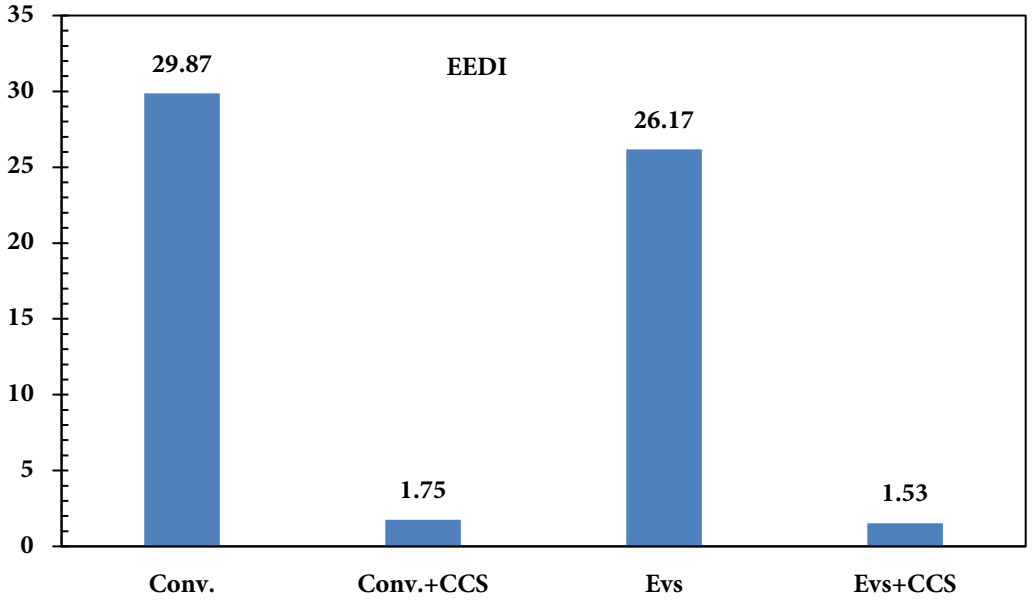

Figure 8. EEDI for variable ship configurations

Table 8. The molar fraction of components in the CCS

Components	Absorber MEA inlet	Absorber Exhaust inlet	Absorber MEA outlet	Absorber Exhaust outlet
H_2O	0.95	0.13	0.9259	0.03
CO_2	0	0.12	0.0288	0.067
N_2	0	0.72	1E-5	0.9245
O_2	0	0.03	7.6E-7	0.0385
MEA	0.048	0	0.0453	0

A CCS absorber is a column with two inputs and two outputs. Marine diesel engines exhaust gas absorber on one side and MEA solution enters the system on the other side. A 20-stage structure has been used throughout the system, and the absorber is based on the process of dissolving CO_2 in the MEA solution by mass transfer. The CO_2 components, which were initially 12% by volume, decreased to approximately 0.67% with a 95% decrease in the absorber output. After mass transfer, the CO_2 in the MEA solution was determined to be approximately 0.0288% by volume. Figure 8 expresses the volumetric ratios of H_2O, CO_2, N_2, O_2, and MEA components in the CCS absorber at the absorber inlet and outlet states.

CO_2 emissions, which cause greenhouse gases on ships, are tried to be reduced with EEDI. There are different options for meeting the IMO's 2050 carbon reduction strategies, these are renewable energy sources, carbon-free fuels, and carbon capture systems. In this study, EEDI calculations were made for four different scenarios. These are configurations that include conventional vehicle-carrying Ro-Ro, electric-vehicle-carrying Ro-Ro, and CCS integration into them. The estimated EEDI for each case is presented in Figure 8. The results show that the use of carbon capture systems on ships can catch up with IMO 2050 strategies. CCS systems reduce the load-carrying capacity of ships and their effects on ship stability are also the main issues to be considered.

The EEDI level of a ship carrying conventional vehicles with CCS was reduced from 29.87 to 1.75, or approximately one-sixteenth. This ratio decreased from 26.17 to 1.53 for electric vehicles and remained approximately the same proportionally.

Conclusion

This study investigated the EEDI effect of stability, hydrostatic, and carbon capture systems installed by IMO by carbon reduction targets for the transport situation of a Ro-Ro ship. According to the ship's design, main engine selection and power requirements were established using appropriate load and resistance calculations. For the chosen equipment and load scenarios, the following results were ultimately obtained.

- According to stability and hydrostatic calculations, the base scenario, which transported conventional vehicles, had the best stability and the scenario involving both EVs and CCS had the lowest stability.
- For both different scenarios, the main engine that can provide the calculations' required power was chosen, and the corresponding speeds for the use of the same engine were established.
- The CO_2 reduction performances of the carbon capture system for Conventional Vehicle transport and EVs transport at different engine loads were evaluated. It was determined that the carbon capture performance increased with increasing MEA solution. It was found that the typical amount of MEA solution to be applied should flow rate around three times that of the exhaust.
- The EEDI value implemented following the IMO carbon reduction targets is highest for conventional vehicles and lowest for EVs with CCS systems. Conclusions reached according to the IMO 2050 objectives; the adoption of CCS reduces CO_2 emissions by almost 95%.

Acknowledgements

This research did not receive any specific grant from funding agencies in the public, commercial, or not-for-profit sectors.

Compliance With Ethical Standards

Authors' Contributions

BG-KB: Designed the study.
BG-KB: Wrote the first draft of the manuscript.
BG-KB: Performed and managed statistical analyses.
Both authors read and approved the final manuscript.

Conflict of Interest

The authors declare that there is no conflict of interest.

Ethical Approval

For this type of study, formal consent is not required.

Data Availability Statement

The data that support the findings of this study are available from the corresponding author upon reasonable request.

References

Ampah, J. D., Yusuf, A. A., Afrane, S., Jin, C., & Liu, H. (2021). Reviewing two decades of cleaner alternative marine fuels: Towards IMO's decarbonization of the maritime transport sector. *Journal of Cleaner Production*, *320*, 128871. https://doi.org/10.1016/j.jclepro.2021.128871

Barrass, B. (2004). *Ship design and performance for masters and mates*. Elsevier.

Bøckmann, E., & Steen, S. (2016). Calculation of EEDI weather for a general cargo vessel. *Ocean Engineering*, *122*, 68-73. https://doi.org/10.1016/j.oceaneng.2016.06.007

Charchalis, A. (2014). Determination of main dimensions and estimation of propulsion power of a ship. *Journal of KONES. Powertrain and Transport*, *21*(2), 39–44. https://doi.org/10.5604/12314005.1133863

Demirel, Y. K., Turan, O., & Incecik, A. (2017). Predicting the effect of biofouling on ship resistance using CFD. *Applied Ocean Research*, *62*, 100–118. https://doi.org/10.1016/j.apor.2016.12.003

Fayaz, H., Saidur, R., Razali, N., Anuar, F. S., Saleman, A. R., & Islam, M. R. (2012). An overview of hydrogen as a vehicle fuel. *Renewable and Sustainable Energy Reviews*, *16*(8), 5511–5528. https://doi.org/https://doi.org/10.1016/j.rser.2012.06.012

Göksu, B., & Bayramoğlu, K. (2021). Control of ship roll and yaw angles during turning motion. *Marine Science and Technology Bulletin*, *10*(4), 340–349. https://doi.org/10.33714/masteb.930338

Grabowska, K., & Szczuko, P. (2015). Ship resistance prediction with Artificial Neural Networks. *2015 Signal Processing: Algorithms, Architectures, Arrangements, and Applications (SPA)*, 168–173. https://doi.org/10.1109/SPA.2015.7365154

Hasan, S. M. R. (2011). *Impact of EEDI on Ship Design and Hydrodynamics: A Study of the Energy Efficiency Design Index and Other Related Emission Control Indexes*. [MSc. Thesis. Chalmers University of Technology].

Holtrop, J., & Mennen, G. G. J. (1982). An approximate power prediction method. *International Shipbuilding Progress*, *29*(335), 166-170.

Ibrahim, R. A., & Grace, I. M. (2010). Modeling of ship roll dynamics and its coupling with heave and pitch. *Mathematical Problems in Engineering*, *2010*, 13–18. https://doi.org/10.1155/2010/934714

Im, N.-K., & Choe, H. (2021). A quantitative methodology for evaluating the ship stability using the index for marine ship intact stability assessment model. *International Journal of Naval Architecture and Ocean Engineering*, *13*, 246–259. https://doi.org/10.1016/j.ijnaoe.2021.01.005

IMO. (2022). Marine Environment Protection Committee (MEPC) – 79th session, 12-16 December 2022.

Irkal, M. A. R., Nallayarasu, S., & Bhattacharyya, S. K. (2016). CFD approach to roll damping of ship with bilge keel with experimental validation. *Applied Ocean Research*, *55*, 1–17. https://doi.org/10.1016/j.apor.2015.11.008

Issa, M., Ilinca, A., & Martini, F. (2022). Ship energy efficiency and maritime sector initiatives to reduce carbon emissions. *Energies*, *15*(21), 7910. https://doi.org/10.3390/en15217910

Jia, J. (2007). Investigations of vehicle securing without lashings for Ro-Ro ships. *Journal of Marine Science and Technology*, *12*(1), 43–57. https://doi.org/10.1007/s00773-006-0240-7

Kafalı, K. (1988). *Gemilerin dizaynı*. İTÜ Baskısı.

Kane, M. (2023). Electric cars from heaviest to lightest. Retrieved on June 5, 2023, from https://insideevs.com/news/527966/electric-cars-from-heaviest-lightest/

Kang, M. H., Choi, H. R., Kim, H. S., & Park, B. J. (2012). Development of a maritime transportation planning support system for car carriers based on genetic algorithm. *Applied Intelligence*, *36*, 585–604. https://doi.org/10.1007/s10489-011-0278-z

Kavli, H. P., Oguz, E., & Tezdogan, T. (2017). A comparative study on the design of an environmentally friendly RoPax ferry using CFD. *Ocean Engineering*, *137*, 22–37. https://doi.org/10.1016/j.oceaneng.2017.03.043

Kennedy, C. (2023). Ro-Ro ferries and the expansion of the PLA's landing ship fleet. Retrieved on June 2, 2023, from https://cimsec.org/ro-ro-ferries-and-the-expansion-of-the-plas-landing-ship-fleet/

Korlak, P. K. (2021). Analysis of operational efficiency of the proposed propulsion systems for selected large ropax vessel. *Nase More*, *68*(3), 199–210. https://doi.org/10.17818/NM/2021/3.7

Kupras, L. K. (1981). Design charts for determining main dimensions, main engine power and building costs of bulkcarriers. *International Shipbuilding Progress*, *28*(322), 136–150.

Kweku, D., Bismark, O., Maxwell, A., Desmond, K., Danso, K., Oti-Mensah, E., Quachie, A., & Adormaa, B. (2017). Greenhouse effect: greenhouse gases and their impact on global warming. *Journal of Scientific Research and Reports*, *17*(6), 1–9. https://doi.org/10.9734/jsrr/2017/39630

Labanti, J., Islam, H., & Guedes Soares, C. (2016). CFD assessment of ropax hull resistance with various initial drafts and trim angles. *Proceedings of 3rd International Conference on Maritime Technology and Engineering, MARTECH 2016*, *1*(October 2017), 325–332. https://doi.org/10.1201/b21890-45

Law, L. C., Othman, M. R., & Mastorakos, E. (2023). Numerical analyses on performance of low carbon containership. *Energy Reports*, *9*, 3440–3457. https://doi.org/10.1016/j.egyr.2023.02.035

Lee, S., Yoo, S., Park, H., Ahn, J., & Chang, D. (2021). Novel methodology for EEDI calculation considering onboard carbon capture and storage system. *International Journal of Greenhouse Gas Control*, *105*, 103241. https://doi.org/10.1016/j.ijggc.2020.103241

Luo, X., & Wang, M. (2017). Study of solvent-based carbon capture for cargo ships through process modelling and simulation. *Applied Energy*, *195*, 402–413. https://doi.org/10.1016/j.apenergy.2017.03.027

MAN. (2014). EEDI energy efficiency design index. Retrieved on October 1, 2014, from https://www.man-es.com/docs/default-source/document-sync-archive/eedi-eng.pdf?sfvrsn=23fbab95_4#:~:text=What%20is%20the%20Energy%20Efficiency,negative%20impact%20on%20the%20environment.

MAN. (2017). Emission project guide. In MAN Energy Solutions. Retrieved on October 1, 2017, from https://man-es.com/applications/projectguides/2stroke/content/special_pg/PG_7020-0145.pdf

Marlantes, K. E., Kim, S. P., & Hurt, L. A. (2022). Implementation of the IMO Second Generation Intact Stability Guidelines. *Journal of Marine Science and Engineering*, *10*, 41. https://doi.org/10.3390/jmse10010041

McClintock, J., Ducklow, H., & Fraser, W. (2008). Ecological responses to climate change on the Antarctic Peninsula. *American Scientist*, *96*(4), 302–310. https://doi.org/10.1511/2008.73.3844

Mihail–Vlad, V. (2018). Advantages and disadvantages of different types of graphs. *Journal of Marine Technology and Environment*, *2*(2), 57.

Mikhaylov, A., Moiseev, N., Aleshin, K., & Burkhardt, T. (2020). Global climate change and greenhouse effect. *Entrepreneurship and Sustainability Issues*, *7*(4), 2897–2913. https://doi.org/10.9770/jesi.2020.7.4(21)

Molland, A. F., Turnock, S. R., & Hudson, D. A. (2017). *Ship resistance and propulsion*. Cambridge University Press.

Mores, P., Rodríguez, N., Scenna, N., & Mussati, S. (2012). CO_2 capture in power plants: Minimization of the investment and operating cost of the post-combustion process using MEA aqueous solution. *International Journal of Greenhouse Gas Control*, *10*, 148–163. https://doi.org/10.1016/j.ijggc.2012.06.002

Mores, P., Scenna, N., & Mussati, S. (2012). A rate based model of a packed column for CO2 absorption using aqueous monoethanolamine solution. *International Journal of Greenhouse Gas Control*, *6*, 21-36. https://doi.org/10.1016/j.ijggc.2011.10.012

Nieuwenhuis, P. (2017). Car Shipping. In A. Beresford & S. Pettit (Eds.), *International Freight Transport: Cases, Structures and Prospects*. Kogan Page.

Niklas, K., & Pruszko, H. (2019). Full-scale CFD simulations for the determination of ship resistance as a rational, alternative method to towing tank experiments. *Ocean Engineering*, *190*, 106435. https://doi.org/10.1016/j.oceaneng.2019.106435

Perissi, I., & Jones, A. (2022). Investigating European Union decarbonization strategies: Evaluating the pathway to carbon neutrality by 2050. *Sustainability*, *14*(8), 4728. https://doi.org/10.3390/su14084728

Perrault, D. (2016). Correlations of GZ curve parameters. *Proceedings of the 15th International Ship Stability Workshop*, Sweden. pp. 1-10.

Polakis, M., Zachariadis, P., & de Kat, J. O. (2019). The energy efficiency design index (EEDI). In Psaraftis, H. (Ed.), *Sustainable shipping*. Springer. https://doi.org/10.1007/978-3-030-04330-8_3

Rutherford, D., Mao, X., & Comer, B. (2020). Potential CO_2 reductions under the Energy Efficiency Existing Ship Index. *International Council on Clean Transportation, Working Paper 2020-27. November 2020*, 1-18.

Sachs, N. M. (2020). The Paris agreement in the 2020s: Breakdown or breakup. *Ecology Law Quarterly*, *46*(3), 865–909. https://doi.org/10.15779/Z38H708140

Salinger, M.J. (2005). Climate variability and change: Past, present and future — an overview. In Salinger, J., Sivakumar, M., & Motha, R. P. (Eds.), *Increasing climate variability and change* (pp. 9-27). Springer. https://doi.org/10.1007/1-4020-4166-7_3

Shakeel, M., Khalid, H., Riaz, Z., Ansari, S. A., & Khan, M. J. (2022). Development of intact stability calculations tool for ships. *Proceedings of 2022 19th International Bhurban Conference on Applied Sciences and Technology*, pp. 858–872. https://doi.org/10.1109/IBCAST54850.2022.9990257

Shepherd, T. A., Zhao, Y., Li, H., Stinn, J. P., Hayes, M. D., & Xin, H. (2015). Environmental assessment of three egg production systems- Part II. Ammonia, greenhouse gas, and particulate matter emissions. *Poultry Science*, *94*(3), 534–543. https://doi.org/10.3382/ps/peu075

Shin, J., & Park, S. (2023). Numerical analysis for optimizing combustion strategy in an ammonia-diesel dual-fuel engine. *Energy Conversion and Management*, *284*, 116980. https://doi.org/10.1016/j.enconman.2023.116980

Simopoulos, G., Konovessis, D., & Vassalos, D. (2008). Sensitivity analysis of the probabilistic damage stability regulations for RoPax vessels. *Journal of Marine Science and Technology*, *13*(2), 164–177. https://doi.org/10.1007/s00773-007-0261-x

Skoupas, S., Zaraphonitis, G., & Papanikolaou, A. (2009). Parametric design and optimization of high-speed, twin-hull roro-passenger vessels. *Proceedings of the 10th International Marine Design Conference*, Norway. pp. 744-760.

Song, L. H., Zhang, Z. G., Wang, X. Z., & Feng, D. K. (2013). Prediction of surface ship's residual resistance coefficient using neural networks. *Advanced Materials Research*, *756–759*, 3141–3144. https://doi.org/10.4028/www.scientific.net/AMR.756-759.3141

Stec, M., Tatarczuk, A., Iluk, T., & Szul, M. (2021). Reducing the energy efficiency design index for ships through a post-combustion carbon capture process. *International Journal of Greenhouse Gas Control*, *108*, 103333. https://doi.org/10.1016/j.ijggc.2021.103333

Sun, X., Wang, S., Wang, Z., Liu, C., & Yin, Y. (2022). A semi-automated approach to stowage planning for Ro-Ro ships. *Ocean Engineering*, *247*, 110648. https://doi.org/10.1016/j.oceaneng.2022.110648

Tadros, M., Ventura, M., & Guedes Soares, C. (2022). Optimization procedures for a twin controllable pitch propeller of a ROPAX ship at minimum fuel consumption. *Journal of Marine Engineering and Technology*, *22*(4), 167-175. https://doi.org/10.1080/20464177.2022.2106623

Thies, F., & Ringsberg, J. W. (2023). Retrofitting WASP to a RoPax vessel—design, performance and uncertainties. *Energies*, *16*(2), 673. https://doi.org/10.3390/en16020673

Tuswan, T., Zubaydi, A., Piscesa, B., Ismail, A., Ariesta, R. C., Ilham, M. F., & Mualim, F. I. (2021). Influence of application of sandwich panel on static and dynamic behaviour of ferry ro-ro ramp door. *Journal of Applied Engineering Science*, *19*(1), 208–216. https://doi.org/10.5937/jaes0-27708

Wang, H., Hou, Y., Xiong, Y., & Liang, X. (2021). Research on multi-interval coupling optimization of ship main dimensions for minimum EEDI. *Ocean Engineering*, *237*, 109588. https://doi.org/10.1016/j.oceaneng.2021.109588

Wang, M., Lawal, A., Stephenson, P., Sidders, J., & Ramshaw, C. (2011). Post-combustion CO_2 capture with chemical absorption: A state-of-the-art review. *Chemical Engineering Research and Design*, *89*(9), 1609–1624. https://doi.org/10.1016/j.cherd.2010.11.005

Xing, H., Spence, S., & Chen, H. (2020). A comprehensive review on countermeasures for CO_2 emissions from ships. *Renewable and Sustainable Energy Reviews*, *134*, 110222. https://doi.org/10.1016/j.rser.2020.110222

Yasukawa, H. (2019). Maneuvering hydrodynamic derivatives and course stability of a ship close to a bank. *Ocean Engineering*, *188*, 106149. https://doi.org/10.1016/j.oceaneng.2019.106149

Zhong, W., & Haigh, J. D. (2013). The greenhouse effect and carbon dioxide. *Weather*, *68*(4), 100–105. https://doi.org/10.1002/wea.2072

Zhou, Y.-M., & Feng, Y.-S. (2014). The strategy and technology selection for non-CO_2 greenhouse gas emission control. *Advances in Climate Change Research*, *5*(1), 28–33. https://doi.org/10.3724/SP.J.1248.2014.028